Geochemical Journal, Vol. 50, pp. 123 to 138, 2016 doi:10.2343/geochemj.2.0395

Terminal Strombolian activity at Etna's central craters during summer 2012: The most CO_2-rich volcanic gas ever recorded at Mount Etna

A. Aiuppa,[1,2]* E. Lo Coco,[1] M. Liuzzo,[2] G. Giudice,[2] G. Giuffrida[2] and R. Moretti[3]

[1]Dipartimento DiSTeM, Università di Palermo, Via Archirafi 36, 90123 Palermo, Italy
[2]Istituto Nazionale di Geofisica e Vulcanologia, Via la Malfa 143, Palermo, Italy
[3]Seconda Università di Napoli, Dipartimento DICDEA, Via Roma, 9, Aversa, Italy

(*Received June 22, 2015; Accepted September 26, 2015*)

By using a permanent network of multi-component gas analyzer systems (Multi-GAS), we report for the first time the H_2O-CO_2-SO_2 composition of the volcanic gases emitted prior to, during, and after terminal Strombolian activity at Mount Etna's central craters (CCs). We show that the summer 2012 Strombolian episodes of the Bocca Nuova crater (BNC), the largest of Etna's CCs, are associated with the emission of the most CO_2-rich gas measured at the volcano thus far. The BNC plume was particularly CO_2-rich with CO_2/SO_2 up to 100, $H_2O/CO_2 < 1$ in the quiescent periods between Strombolian episodes. However, more CO_2-poor gas with $CO_2/SO_2 < 27$, $H_2O/CO_2 > 1$ prevailed at the BNC and at other degassing vents such as Voragine and Northeast craters during Strombolian eruptions. Based on the results of numerical simulations of volcanic degassing, conclude that the shallow Etna plumbing system was invaded in summer 2012 by a CO_2-rich gas front likely supplied by the deep (>100 MPa pressure) volcano's magmatic storage zone. This deep gas-bubble supply eventually caused a general rejuvenation of the resident magma in the upper conduits/shallow reservoirs, thereby triggering the first Strombolian episodes on the volcano's summit after years of quiescence.

Keywords: volcanic gases, Etna, volcanic degassing, Multi-GAS, volcano monitoring

Introduction

Mount Etna (Italy), one of the most studied and closely monitored volcanoes in the world (Bonaccorso *et al*., 2004), has long been regarded as a prodigious source of magmatic gas via persistent degassing through its active summit craters and upper flanks (Allard *et al*., 1991, 2006; Gerlach, 1991; Caltabiano *et al*., 2004; Aiuppa *et al*., 2006, 2008). Etna's gas emissions have been studied by using a variety of techniques including airborne plume profiling (Allard *et al*., 1991), Fourier transform infrared spectroscopy (FTIR) during passive degassing (Francis *et al*., 1998) and lava fountains (Allard *et al*., 2005; La Spina *et al*., 2015), direct sampling (e.g., Aiuppa *et al*., 2004; Martelli *et al*., 2008; Paonita *et al*., 2012), and, more recently, the multi-component gas analyzer system (Multi-GAS) technique. Since its advent in the middle of the last decade, Multi-GAS has enabled improved, direct in situ observations of Etna's volcanic gas plumes, allowing the acquisition of unprecedented long time-series of plume CO_2/SO_2 ratio compositions (Aiuppa *et al*., 2006, 2007). Multi-GAS has also been established as an inexpensive and powerful tool for in situ simultaneous sensing of other major and trace volcanogenic components in volcanic gas plumes such as H_2O (Aiuppa *et al*., 2008; Shinohara *et al*., 2008) and H_2 and H_2S (Aiuppa *et al*., 2011), respectively. This, combined with the refinement of thermodynamic saturation codes (Moretti and Papale, 2004), has enabled more detailed inspection of the degassing processes and a better interpretation of the transition from quiescence to eruption (Aiuppa *et al*., 2007, 2010a, b).

The network of permanent Multi-GAS instruments, run by the Istituto Nazionale de Geofisica e Vulcanologia (INGV), currently includes three fully automated instruments located on the rims of the Voragine (VOR), Bocca Nuova (BNC), and Northeast (NEC) summit craters (Fig. 1). These three craters, which had erupted recurrently during the 1995–2002 eruptive cycle (Allard *et al*., 2006), have remained quiescent since 2006, when the permanent Multi-GAS instruments began operation. Although an abundance of Multi-GAS information is available on the passive signature of magmatic gases, the present study is the first to present data associated with the explosive episodes of these craters.

After several years of dormancy, mild Strombolian activity resumed within Etna's BNC in July 2012 (Pering *et al*., 2015). This Strombolian activity, which persisted

*Corresponding author (e-mail: alessandro.aiuppa@unipa.it)

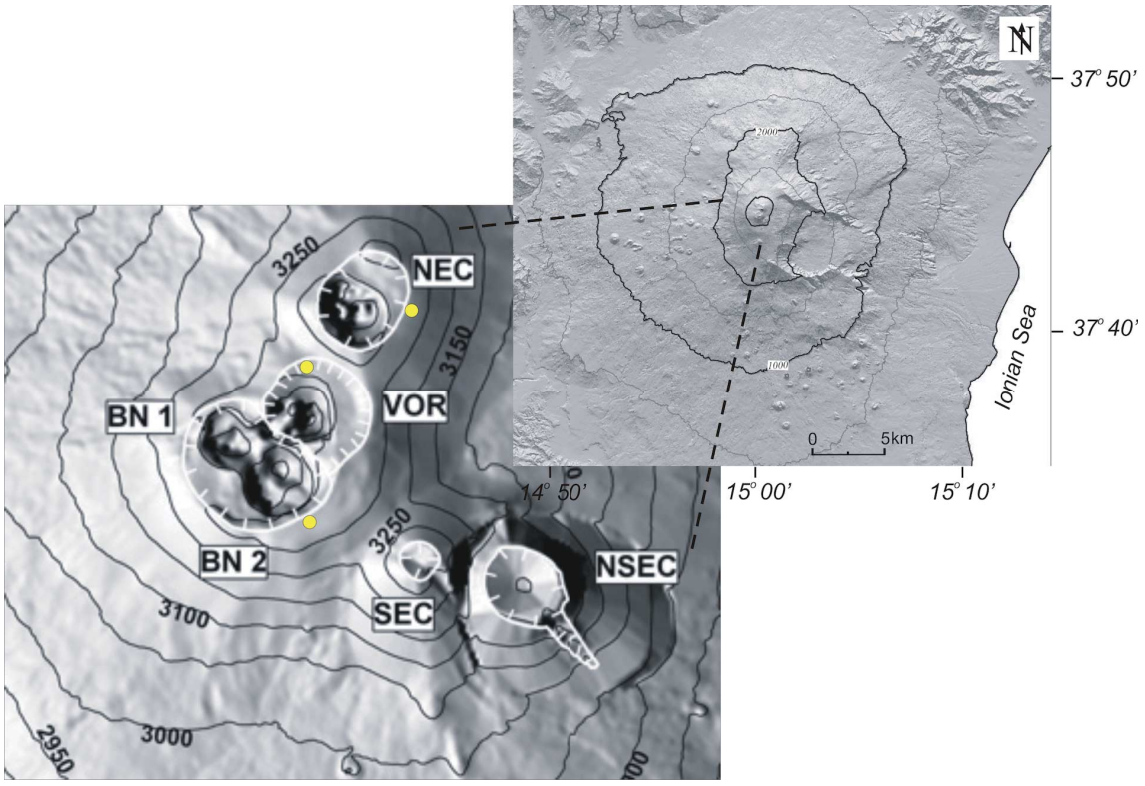

Fig. 1. Digital elevation map of the Etna summit, courtesy of the Istituto Nazionale de Geofisica e Vulcanologia-Osservatorio Etneo (INGV-OE). Locations of the permanent multi-component gas analyzer system (Multi-GAS) instruments are represented by yellow dots.

intermittently during July–August and October 2012, offered the first opportunity to investigate the compositional features of gases emitted during the pre-, syn- and post-eruptive phases of the BNC. Herein, we describe the results of such Multi-GAS observations to determine the H_2O, CO_2, and SO_2 compositions of July–December 2012 activity. These results are then used to derive new constraints on the mechanisms of the magmatic supply and ascent beneath the shallow conduit region of the Etna volcano. Further, we compare our volcanic gas data with the results obtained by the Moretti and Papale (2004) equilibrium saturation model, which we use to numerically reproduce the degassing trends of Etna's magma upon its ascent and decompression. Overall, the results presented in this study enable an improved understanding of Etna's plumbing system.

Brief Summary of Volcanic Activity

Etna's BNC resumed its explosive activity during summer–fall 2012 (Fig. 2). Since its formation in the 1960s, the BNC has frequently undergone intense periods of prolonged Strombolian activity often accompanied by emission of small lava flows on the crater floor. The most recent of these periods occurred between July 1995 and early 2001, when the crater gradually filled through the growth of pyroclastic cones and intra-crateric lava outpouring to overflow several times between October and November 1999 (Allard *et al*., 2006, and references cited therein). No magmatic activity has been observed at the BNC since 2001, with the exception of a moderate lava flow episode from the base of the crater in 2006 (Bonforte *et al*., 2008; Behncke *et al*., 2009).

On the evening of July 2, 2012, modest intra-crateric Strombolian activity began at the BNC, as reported on the INGV-Osservatorio Etneo (INGV-OE) (website at http://www.ct.ingv.it/it/). This activity continued, albeit irregularly, until October 2012 and occurred in the following three distinct phases.

Phase 1: Continuous activity, July 2–24, 2012

According to INGV-OE reports, Strombolian activity was nearly continuous inside the BNC during July 2–24, 2014. On July 8, a small lava flow field was observed on the flanks of the pyroclastic cone that formed on the bottom of the BNC. This activity continued with similar characteristics until July 24, when a dramatic drop in volcanic tremor amplitude coincided with a sudden decrease in eruption intensity. During the subsequent days, frequent small-ash emissions were observed, likely owing to small

Fig. 2. Strombolian activity inside the Bocca Nuova crater (BNC) during summer 2012 (photo courtesy of F. Ciancitto).

collapses inside the feeding conduit at the summit of the new cone. Unfortunately, this part of the eruption occurred during a non-functional term of Multi-GAS during the winter period and was hence not monitored. Recording resumed on July 27.

Phase 2: Episodic activity, July 26–August 25, 2012
Episode 1: July 26–27, 2012 On the morning of July 26, Strombolian activity resumed inside the BNC, with characteristics similar to those in the July 2–24 episodes. These eruptions were accompanied by the emission of a lava flow from an effusive vent located on the western portion of the crater's bottom. Eruption dynamics and SO_2 budgets for individual eruptions were characterized on July 27 by Pering *et al.* (2015). On the same day, the depression in the central well at the bottom of the BNC was almost completely filled with lava. The eruptive activity progressively declined and ceased during the evening.
Episode 2: July 29–August 1, 2012 After a single day of inactivity on July 28, during which time several ash emissions were observed, eruptive activity resumed on July 29 including small Strombolian eruptions and lava emissions from a vent located on the southern flank of the pyroclastic cone on the BNC's bottom. This new episode ended on August 1.
Episode 3: August 3–4, 2012 A new episode of Strombolian activity began on August 3 and was accompanied by lava emissions on the crater floor. Activity reached peak intensity around midnight, decreased on the morning of August 4, and ceased later that evening. This episode was followed by small ash puffs, which signified weak explosive activity remaining in the BNC.
Episode 4: August 6–7, 2012 The fourth episode began on the afternoon of August 6 and showed the same characteristics as those of previous episodes. The activity peaked just before midnight and ceased during the afternoon of August 7. Sporadic ash emissions, clearly associated with eruptions, characterized the subsequent period of relative quiescence. A survey conducted August 9 by INGV-OE staff members demonstrated that the summit of new intra-pyroclastic cone crater experienced a partial collapse, likely caused by a drop in the magma column inside the conduit.
Episode 5: August 10–11, 2012 Similar to that shown in previous episodes, the beginning of the fifth episode was marked by a sudden increase in amplitude of the volcanic tremor. A strong glow inside the crater was visible on the evening of August 10 from tens of kilometers away. Incandescent pyroclastic materials were launched well above the crater rim. Activity ceased during the morning of August 11. Ash emissions were particularly frequent on August 13 and continued until August 25.

Phase 3: Continuous activity, October 2–7, 2012

On the evening of October 2, Strombolian activity was observed again at the BNC. Beginning on October 3, this activity was accompanied by emissions of small intracrateric lava flows directed southward. On the evening of October 6, a sudden increase occurred in the amplitude of the volcanic tremor, and the eruptive activity in-

tensified. Emission of a well-fed lava flow was directed toward the center of the crater depression, and vigorous Strombolian activity at times assumed the characteristics of a lava fountain. Both the intensity of the eruption and the amplitude of the volcanic tremor peaked shortly after midnight on October 7 and began to decline about 3 h later.

METHODOLOGY

The CO_2/SO_2 and H_2O/CO_2 ratios in the volcanic gas plume were measured by using three permanent INGV-Pa Multi-GAS instruments (Aiuppa *et al*., 2007) located on the outer rims of the active vents at the following Global Positioning System (GPS) coordinates: BNC, 14.99113°E, 37.74796°N; VOR, 14.99493°E, 37.75153°N; and NEC, 14.99708°E, 37.75283°N; Fig. 1).

Multi-GAS is a combination of various gas analyzers that simultaneously measure the concentrations of gaseous species in a volcanic plume. This instrument typically records the CO_2 and SO_2 concentrations in a volcanic plume in real-time through the integration of an infrared spectrometer and a specific electrochemical sensor for CO_2 and SO_2 measurement. For CO_2 measurement, the Gascard II model, Edinburgh Sensors, was used with a 0–3000 ppmv calibration range, ±2% accuracy, 0.8 ppmv resolution, 0–45°C operating temperature, 800–1150 mbar operating pressure, and 24 V DC, 7–30 V power requirements. For SO_2 measurement, a specific electrochemical sensor (3ST/F, Cod TD2D-1A model, City Technology, Ltd) was used with a 0–200 ppmv calibration range, 2% accuracy, –20°C to +50°C operating temperature, and atm ±10% operating pressure. According to the manufacturer's datasheet, the 3ST/F sensor resolution is 0.5 ppmv, and the true detection limit with the 16-bit digitizer onboard the Multi-GAS is 10 ppbv. The H_2O concentrations in the plume were obtained from measured relative humidity (Rh), air temperature (°C) and pressure (mbar) based on the Arden Buck equation:

$$H_2O\ [ppm] = \{6.1121 \times (1.0007 + 3.46 \times p^{-6}) \times \exp[(17.502 \times T)/(240.97 + T)] \times Rh/100 \times 10^6\}/P. \quad (1)$$

Because the plume is a mixture of volcanic and atmospheric gases, the original magmatic gas composition prior to atmospheric dilution can be estimated from correlations of co-acquired gas species (Aiuppa *et al*., 2006). In our specific case, post-processing involved the following steps: (Aiuppa *et al*., 2014): (i) subtraction of CO_2 and H_2O concentrations in the background air, which was achieved by fitting the polynomial curves to the minima in the original CO_2 and H_2O time series (e.g., to the CO_2 and H_2O datapoints that correspond to an SO_2 level of ~0 ppmv); (ii) calculation of 30-min averages of volcanic CO_2/SO_2 and H_2O/CO_2 ratios, which were obtained from the slopes of linear regression lines in CO_{2corr} versus SO_2 and H_2O_{corr} versus CO_{2corr} scatter diagrams, where H_2O_{corr} and CO_{2corr} are background air-corrected CO_2 and H_2O concentrations, respectively. Examples of scatter plots for both CO_2-rich and CO_2-poor plumes are given in Figs. 3a and b. This calculation routine was automated by using Ratiocalc software (Tamburello, 2015). A measurement cycle was considered null (i.e., no ratio was calculated) when SO_2 concentrations were below a specific threshold value of <5 ppm; this condition occurred in case of unfavorable wind transport directions. In such dilute plume conditions, the procedure of subtracting the background air CO_2 concentrations becomes more complex and often leads to the overestimation of actual volcanic gas CO_2/SO_2 ratios. Laboratory tests with standard gas mixtures demonstrated a maximum uncertainty in the derived CO_2/SO_2 ratios of 15% (Pering *et al*., 2014), whereas the error, expressed as one standard deviation, in individually derived H_2O/CO_2 ratios was ≤25%.

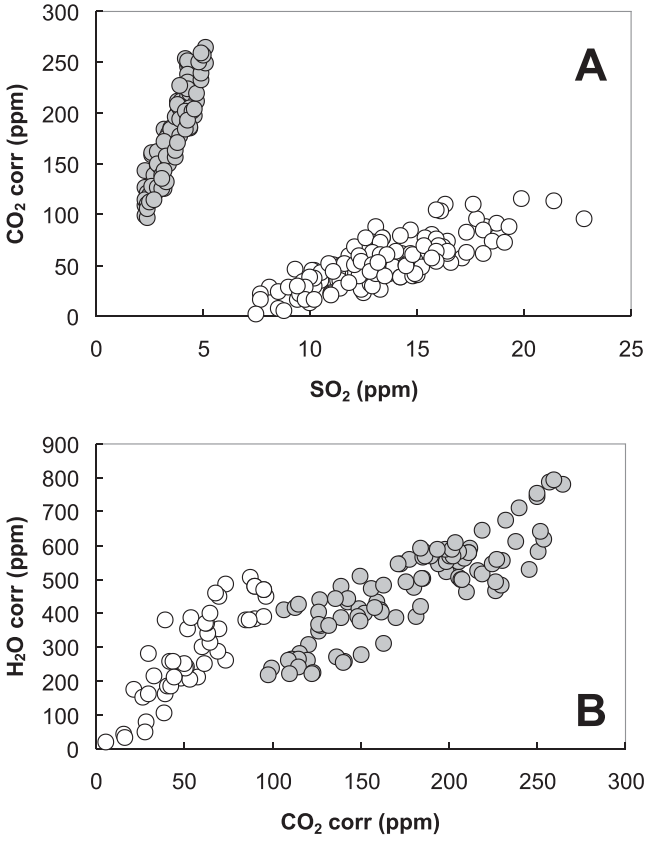

Fig. 3. Examples of scatter plots of a) CO_{2corr} versus SO_2 and b) H_2O_{corr} versus CO_{2corr} for high-CO_2 (gray symbols) and low-CO_2 (open symbols) volcanic gas plumes, respectively. H_2O_{corr} and CO_{2corr} are background air-corrected CO_2 and H_2O concentrations in the plume, respectively.

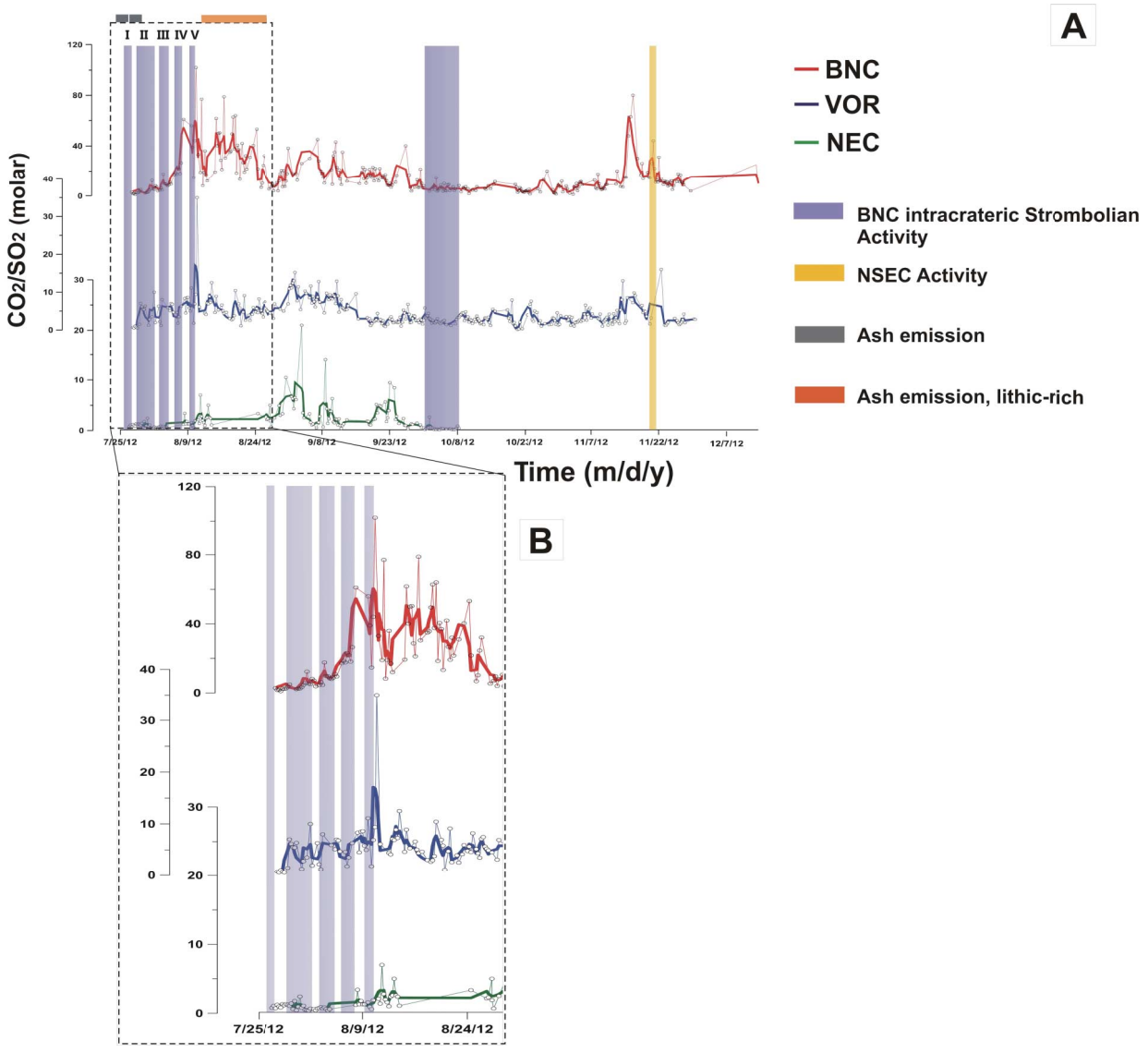

Fig. 4. a) Time series of molar CO_2/SO_2 ratios in the plumes of Etna's summit craters during summer 2012. The chronology of the main volcanic events is indicated by colored bars, as obtained by the Istituto Nazionale de Geofisica e Vulcanologia-Osservatorio Etneo (INGV-OE) monitoring reports available at http://www.ct.ingv.it/it/ A zoom of the July–August period is given in b).

Results

The derived CO_2/SO_2 and H_2O/CO_2 molar ratios for each measurement interval and crater are listed in Table 1. Both ratios exhibited large variations during the investigatory period and ranged from 0.1 to 102 and from 0.51 to 117, respectively. Similar to previous studies (Aiuppa *et al.*, 2006, 2011; Shinohara *et al.*, 2008; La Spina *et al.*, 2010), distinct compositions were observed at the three craters, with plume gases becoming more CO_2-depleted in the sequence of BNC, VOR, NEC (Fig. 4). The mean (±1 standard deviation) CO_2/SO_2 ratios for individual craters were BNC, 15.5 ± 15 (range: 1–102); VOR. 4.5 ± 3.1 (range: 0.1–35); and NEC, 2.1 ± 2.6 (range: 0.15–21). The H_2O/CO_2 averages were BNC, 3.6 ± 2.5 (range: 0.5–17.4); VOR, 14.3 ± 14.6 (range: 0.8–117); and NEC, 13 ± 10 (range: 1.3–52; Table 1).

Figure 3 shows a time series of the CO_2/SO_2 ratios for the three individual craters. The diagram demonstrates that temporal fluctuations in gas compositions generally responded to variations in volcanic activity. CO_2/SO_2 ratios at BNC were generally lower during eruptive intervals than during periods of quiescent degassing. In particular, the periods of intra-crateric Strombolian activity were associated with plume CO_2/SO_2 ratios of 1.7–26.5, with an average value of 8.5 ± 6. This value is lower than

Table 1. Molar CO_2/SO_2 and H_2O/CO_2 in the near-vent plumes of Bocca Nuova (BNC) Voragine (VOR), and Northeast (NEC) craters of Mount Etna. Each value represents the time-averaged ratio for a measurement interval of 30 min during which time measurements were taken by the multi-component gas analyzer system (Multi-GAS) every 9 s. The date is the starting time of each acquisition interval; the time is local time.

Date	CO_2/SO_2			H_2O/CO_2			Date	CO_2/SO_2			H_2O/CO_2		
	VOR	BN	NEC	VOR	BN	NEC		VOR	BN	NEC	VOR	BN	NEC
27/07/2012 1.00			0.8				22/08/2012 13.00	3.9			8.6		
27/07/2012 7.00			1.1			17.8	22/08/2012 19.00	2.5	31.0		19.3		
27/07/2012 13.00		2.8	0.7		9.6		23/08/2012 7.00	4.1			29.2		
27/07/2012 19.00	0.7	1.7	1.2		5.9	9.8	23/08/2012 13.00	5.9	40.3		17.1	1.3	
28/07/2012 1.00	0.5	1.8	1.0	22.6	3.7	9.2	24/08/2012 1.00	4.8					
28/07/2012 7.00	1.0	1.0	0.8	23.5	7.3		24/08/2012 7.00	5.6	53.2		8.4	2.5	
28/07/2012 13.00	0.7	2.4	1.3	17.1	16.3		24/08/2012 13.00	4.6	21.7	3.4		3.2	
28/07/2012 19.00	0.5	2.3	1.2		5.5	21.7	24/08/2012 19.00	8.2			3.3		
29/07/2012 1.00		2.6	1.3		1.9		25/08/2012 7.00	5.2	6.8		5.7	6.9	
29/07/2012 7.00	1.5	3.6	1.2		10.1		25/08/2012 13.00	4.3	10.2		18.8	2.1	
29/07/2012 13.00	7.0	4.9	1.1	12.5	10.6	10.2	25/08/2012 19.00	3.5	24.5		10.7	2.1	
29/07/2012 19.00	6.1		1.4				26/08/2012 1.00	7.1	32.1			1.3	
30/07/2012 1.00	5.5		0.6	2.6			26/08/2012 7.00	7.5	5.4				
30/07/2012 7.00	5.4		1.8	4.3			26/08/2012 13.00	5.6					
30/07/2012 13.00	6.4	2.1	0.4	5.7	8.8	1.7	26/08/2012 19.00	5.2	7.0	2.2			
30/07/2012 19.00		2.5	1.0		4.8		27/08/2012 1.00	4.9	9.6	2.3			
31/07/2012 1.00		2.5	2.4		4.0		27/08/2012 7.00		4.0				
31/07/2012 7.00	1.3	3.3	0.8	17.2	4.1		27/08/2012 13.00	4.5	7.9	1.9	20.9		35.5
31/07/2012 13.00	2.8	4.6	1.1	10.7	17.4	5.6	27/08/2012 19.00			0.7			6.8
31/07/2012 19.00		5.7	0.5		4.8	7.1	28/08/2012 7.00	3.1			10.8	6.5	
01/08/2012 1.00	3.5	12.3	0.4	1.7	3.5		28/08/2012 13.00	6.9		2.5	47.9	4.8	14.2
01/08/2012 7.00		5.4	0.4		3.8	3.8	29/08/2012 1.00		10.5			1.4	
01/08/2012 13.00	10.0	5.0	0.7	7.6	6.4	18.2	29/08/2012 7.00		3.9				
01/08/2012 19.00	1.9	8.1		14.8	2.8		29/08/2012 13.00		11.9	4.9		5.2	
02/08/2012 1.00		7.1	0.6		3.9		29/08/2012 19.00	5.5	18.0	3.0	3.3	3.6	2.3
02/08/2012 7.00		3.8	0.4		2.0		30/08/2012 1.00		20.5			1.9	
02/08/2012 13.00	6.3		0.7	3.7		52.5	30/08/2012 7.00		7.3	3.3		7.7	
02/08/2012 19.00	2.2	4.5	0.8	31.9	3.2	4.3	30/08/2012 13.00	5.0	20.4		16.3	1.4	
03/08/2012 1.00	1.2	6.2	0.9	4.2	3.5		30/08/2012 19.00		7.5				
03/08/2012 7.00	8.0	4.6	0.7		6.6	6.9	31/08/2012 1.00		11.7	10.5			
03/08/2012 13.00		17.6	0.9		5.8		31/08/2012 7.00		18.0			1.3	
03/08/2012 19.00		9.7	0.6		3.5		31/08/2012 13.00	6.9	38.1		15.1		
04/08/2012 1.00		9.6	0.4		2.6	4.8	31/08/2012 19.00	10.9			7.2		
04/08/2012 7.00		8.4	0.6		4.2		01/09/2012 1.00	11.8			5.9		
04/08/2012 13.00	5.9	8.0		26.2	5.6		01/09/2012 7.00	11.1		6.7	11.7		
04/08/2012 19.00		8.8			3.0		01/09/2012 13.00	12.4	18.0	6.3			6.0
05/08/2012 1.00	5.1	10.9			3.0		01/09/2012 19.00	13.0		4.3			14.3
05/08/2012 7.00	7.0	9.5		11.7	3.1		02/09/2012 1.00	15.2		6.5			20.4
05/08/2012 13.00	6.8			7.4			02/09/2012 7.00		18.0	6.1		3.4	17.3
05/08/2012 19.00	4.7			2.2			02/09/2012 13.00	7.7	12.6		15.5	1.9	
06/08/2012 1.00		17.2			3.7		02/09/2012 19.00	11.4					
06/08/2012 7.00		18.5			3.2		03/09/2012 7.00	5.4					
06/08/2012 13.00	4.6	17.6		11.4	2.2		03/09/2012 13.00		26.0	21.0		3.9	
06/08/2012 19.00	1.8	23.1			4.0		03/09/2012 19.00			3.5			20.7
07/08/2012 1.00	3.5	21.8		17.0	3.4		04/09/2012 1.00			2.5			
07/08/2012 7.00		18.1			5.5		04/09/2012 7.00	10.3			18.5		
07/08/2012 13.00	6.3	26.5		9.9	1.9		04/09/2012 13.00	9.7			8.5		
08/08/2012 1.00		61.0	1.2		2.7		05/09/2012 7.00	8.5	30.0	3.3	7.5	1.0	17.6
08/08/2012 7.00	8.3		3.4	7.3		2.4	05/09/2012 13.00	11.6		1.6			
08/08/2012 13.00	4.5		1.3				05/09/2012 19.00	7.1		1.1	1.7		
08/08/2012 19.00	8.5		1.8	2.4		24.6	06/09/2012 1.00	8.9		1.3			
09/08/2012 1.00	8.6		1.3	21.0			06/09/2012 7.00	7.5			10.1		
09/08/2012 7.00	5.8		1.3	11.2		29.8	06/09/2012 13.00	6.1			9.3		
09/08/2012 13.00	5.0			5.1			06/09/2012 19.00	8.0		0.5			
09/08/2012 19.00	11.1	56.0	1.6	3.1	0.7		07/09/2012 1.00	8.7	45.0		10.0		
10/08/2012 1.00		39.0	0.9		1.5		07/09/2012 7.00	12.8	28.0	1.6		2.4	
10/08/2012 7.00	1.8	14.7	0.6	8.5	6.1		07/09/2012 13.00	7.4		2.8	16.3		
10/08/2012 13.00	6.9	44.0	1.9		2.0	37.2	07/09/2012 19.00		20.0			2.0	
10/08/2012 19.00	9.4	102.0			2.4		08/09/2012 1.00		18.0			0.7	

Table 1. (continued)

Date	CO_2/SO_2			H_2O/CO_2			Date	CO_2/SO_2			H_2O/CO_2		
	VOR	BN	NEC	VOR	BN	NEC		VOR	BN	NEC	VOR	BN	NEC
11/08/2012 1.00	35.0						08/09/2012 7.00		15.0	0.7		0.9	
11/08/2012 7.00		33.0	2.1		1.1	4.3	08/09/2012 13.00	4.5	10.3			4.2	
11/08/2012 13.00	6.1		1.4	0.9			08/09/2012 19.00			14.0			
11/08/2012 19.00		19.0	7.0		1.8		09/09/2012 1.00	9.7		4.3	7.3		
12/08/2012 1.00		77.0	2.8		0.5		09/09/2012 7.00			1.4			
12/08/2012 7.00		8.2	2.0		2.4		09/09/2012 13.00	8.0		2.3	25.3		
12/08/2012 13.00		19.0	1.6		4.2		09/09/2012 19.00	9.3		3.8			
12/08/2012 19.00	4.4	36.0	1.0	12.8	3.7		10/09/2012 1.00	8.3	21.0	3.8	16.1		
13/08/2012 1.00	4.1	17.0	2.4		2.5	14.0	10/09/2012 7.00	8.2	9.3	6.3	4.5	3.8	
13/08/2012 7.00	7.1	12.0	2.6	13.4	6.3		10/09/2012 13.00	9.2	32.0	1.7	9.2		
13/08/2012 13.00	6.9		5.0	8.7		18.1	10/09/2012 19.00	8.9	35.0	1.5		1.6	
13/08/2012 19.00	8.9		2.6				11/09/2012 1.00	7.0	43.0	2.3		0.8	
14/08/2012 1.00	7.3		2.4				11/09/2012 7.00	12.9	23.0	2.2	1.1		7.0
14/08/2012 7.00	12.5		1.1				11/09/2012 13.00	9.0		1.1	13.0		12.7
15/08/2012 1.00	4.6	19.3			5.1		11/09/2012 19.00	4.7	21.0	2.3		3.8	
15/08/2012 7.00	8.9	61.7		4.9	1.3		12/09/2012 1.00		13.3	1.0			
15/08/2012 13.00		40.1			5.1		12/09/2012 7.00	8.0	9.0	0.4		1.9	
15/08/2012 19.00	5.3	49.9		10.9	2.5		12/09/2012 13.00	5.9	35.0	1.0			22.3
16/08/2012 1.00		50.3			3.2		12/09/2012 19.00	5.7		1.3			
16/08/2012 7.00		28.7			3.4		13/09/2012 1.00	5.3			3.6		
16/08/2012 13.00	6.6	21.2		14.4	8.0		13/09/2012 7.00	5.4					
16/08/2012 19.00	5.1			4.5			13/09/2012 13.00	5.4	11.7	2.1			14.3
17/08/2012 1.00	4.4	78.8		12.0	3.5		13/09/2012 19.00	6.4					
17/08/2012 7.00		30.4			2.3		15/09/2012 13.00	9.6			9.9		
17/08/2012 13.00	4.6			12.3			16/09/2012 1.00	2.9			1.6		
18/08/2012 7.00	3.0	34.9			2.2		16/09/2012 7.00		9.9				
18/08/2012 13.00		35.7			3.6		16/09/2012 19.00		19.0				
18/08/2012 19.00	2.7	49.5		9.1	1.6		17/09/2012 1.00		22.9				
19/08/2012 1.00	3.0	62.8			1.1		17/09/2012 7.00		13.8			4.1	
19/08/2012 7.00	3.8	37.6		19.1			17/09/2012 13.00		21.2				
19/08/2012 13.00	10.4	64.0		10.6	2.4		17/09/2012 19.00		10.2			5.1	
19/08/2012 19.00		18.5			1.6		18/09/2012 1.00	3.2	14.4	1.9	1.4	3.6	
20/08/2012 1.00		40.5			0.5		18/09/2012 7.00	2.8	16.1	1.8		2.4	
20/08/2012 7.00	6.9	37.0			1.3		18/09/2012 13.00	3.0	21.3	1.1			
20/08/2012 13.00	5.8	13.3		27.4	3.5		18/09/2012 19.00	1.2	16.3	1.1	2.9		
20/08/2012 19.00	1.1			2.8			19/09/2012 1.00	1.7	14.7		2.5	0.8	
21/08/2012 1.00		41.9			1.9		19/09/2012 7.00	2.5	23.0			3.4	
21/08/2012 7.00	4.7	26.7		25.2	3.0		19/09/2012 13.00	2.2	11.9	2.2			
21/08/2012 13.00	9.1	19.2		11.6	2.1		19/09/2012 19.00	2.4	21.9	2.3		2.8	
21/08/2012 19.00	2.6	32.0					20/09/2012 1.00	2.7		5.2			
22/08/2012 1.00		21.6					20/09/2012 7.00	4.4	14.2	3.5		3.0	
21/09/2012 7.00			0.8				20/10/2012 1.00	7.9			2.4		
21/09/2012 13.00			1.1			17.8	20/10/2012 7.00	1.7			3.1		
21/09/2012 19.00		2.8	0.7		9.6		20/10/2012 13.00	2.0			31.9		
22/09/2012 1.00	0.7	1.7	1.2		5.9	9.8	20/10/2012 19.00	1.1	9.2		2.3		
22/09/2012 7.00	0.5	1.8	1.0	22.6	3.7	9.2	21/10/2012 1.00		7.0			2.2	
22/09/2012 13.00	1.0	1.0	0.8	23.5	7.3		21/10/2012 7.00	0.1	2.7				
22/09/2012 19.00	0.7	2.4	1.3	17.1	16.3		21/10/2012 13.00	0.3	3.8				
23/09/2012 1.00	0.5	2.3	1.2		5.5	21.8	21/10/2012 19.00	2.1	6.3				
23/09/2012 7.00		2.6	1.3		1.9		22/10/2012 1.00		5.5				
23/09/2012 13.00	1.5	3.6	1.2		10.1		22/10/2012 7.00	0.3	3.6				
23/09/2012 19.00	7.0	4.9	1.1	12.5	10.6	10.2	22/10/2012 13.00		3.0				
24/09/2012 1.00	6.1		1.4				22/10/2012 19.00		2.8				
24/09/2012 7.00	5.5		0.6	2.6			23/10/2012 1.00		3.9				
24/09/2012 13.00	5.4		1.8	4.3			23/10/2012 7.00		3.8			3.4	
24/09/2012 19.00	6.4	2.1	0.4	5.7	8.8	1.7	23/10/2012 13.00	4.0	4.7		18.3		
25/09/2012 1.00		2.5	1.0		4.8		23/10/2012 19.00		2.3				
25/09/2012 7.00		2.5	2.4		4.0		24/10/2012 1.00		2.7				
25/09/2012 13.00	1.3	3.3	0.8	17.2	4.1		24/10/2012 7.00		5.2				
25/09/2012 19.00	2.8	4.6	1.1	10.7	17.4	5.6	24/10/2012 13.00	6.8	1.5		6.9		
26/09/2012 1.00		5.7	0.5		4.8	7.1	24/10/2012 19.00	7.6					

Table 1. (continued)

Date	CO_2/SO_2			H_2O/CO_2			Date	CO_2/SO_2			H_2O/CO_2		
	VOR	BN	NEC	VOR	BN	NEC		VOR	BN	NEC	VOR	BN	NEC
26/09/2012 7.00	3.5	12.3	0.4	1.7	3.5		25/10/2012 1.00	2.7			7.2		
26/09/2012 13.00		5.4	0.4		3.8	3.8	25/10/2012 7.00	2.3					
27/09/2012 1.00	10.0	5.0	0.7	7.6	6.4	18.2	25/10/2012 13.00	5.0			9.7		
27/09/2012 7.00	1.9	8.1		14.8	2.8		26/10/2012 1.00	4.6					
27/09/2012 13.00		7.1	0.6		3.9		26/10/2012 7.00		5.5				
27/09/2012 19.00		3.8	0.4		2.0		26/10/2012 13.00	1.8					
28/09/2012 1.00	6.3		0.7	3.7		52.5	26/10/2012 19.00	2.4	3.1				
28/09/2012 7.00	2.2	4.5	0.8	31.9	3.2	4.3	27/10/2012 1.00	1.0			56.3		
28/09/2012 13.00	1.2	6.2	0.9	4.2	3.5		27/10/2012 13.00		13.0			3.5	
28/09/2012 19.00	8.0	4.6	0.7		6.6	6.9	27/10/2012 19.00	1.7			51.8		
29/09/2012 1.00		17.6	0.9		5.8		28/10/2012 7.00		20.0				
29/09/2012 7.00		9.7	0.6		3.5		28/10/2012 19.00	1.4					
29/09/2012 13.00		9.6	0.4		2.6	4.8	29/10/2012 7.00	1.5					
29/09/2012 19.00		8.4	0.6		4.2		29/10/2012 13.00	3.2	4.9				
30/09/2012 1.00	5.9	8.0		26.2	5.6		29/10/2012 19.00	3.1	2.6				
30/09/2012 7.00		8.8			3.0		30/10/2012 1.00	2.5	2.4				
30/09/2012 13.00	5.1	10.9			3.0		30/10/2012 7.00	1.5	1.5				
30/09/2012 19.00	7.0	9.5		11.7	3.1		30/10/2012 13.00	4.5					
01/10/2012 1.00	6.8			7.4			30/10/2012 19.00	1.3	8.5		10.1		
01/10/2012 7.00	4.7			2.2			31/10/2012 1.00	1.5	7.4		5.4		
01/10/2012 13.00		17.2			3.7		31/10/2012 7.00	3.8			55.4		
01/10/2012 19.00		18.5			3.2		31/10/2012 13.00		11.7				
02/10/2012 1.00	4.6	17.6		11.4	2.2		31/10/2012 19.00		3.2				
02/10/2012 7.00	1.8	23.1			4.0		01/11/2012 13.00	3.5	7.8		34.7		
02/10/2012 13.00	3.5	21.8		17.0	3.4		01/11/2012 19.00	2.4	5.5				
02/10/2012 19.00		18.1			5.5		02/11/2012 1.00	2.7					
03/10/2012 1.00	6.3	26.5		9.9	1.9		02/11/2012 7.00	3.6	2.2		1.4		
03/10/2012 7.00		61.0	1.2		2.7		02/11/2012 13.00	1.2					
03/10/2012 13.00	8.3		3.4	7.3		2.4	02/11/2012 19.00	3.3			1.3		
03/10/2012 19.00	4.5		1.3				03/11/2012 1.00	1.5	1.3				
04/10/2012 1.00	8.5		1.8	2.4		24.6	03/11/2012 7.00	1.0	7.2				
04/10/2012 7.00	8.6		1.3	21.0			03/11/2012 13.00	1.9	5.5				
04/10/2012 13.00	5.8		1.3	11.2		29.8	03/11/2012 19.00		9.9				
04/10/2012 19.00	5.0			5.1			04/11/2012 1.00	2.1	4.1		13.2		
05/10/2012 1.00	11.1	56.0	1.6	3.1	0.7		04/11/2012 7.00	2.4	7.1		16.5		
05/10/2012 7.00		39.0	0.9		1.5		04/11/2012 13.00	2.7	10.8				
05/10/2012 13.00	1.8	14.7	0.6	8.5	6.1		04/11/2012 19.00	2.3	11.4				
05/10/2012 19.00	6.9	44.0	1.9		2.0	37.2	05/11/2012 1.00	2.7	9.0				
06/10/2012 1.00	9.4	102.0			2.4		05/11/2012 7.00	2.6					
06/10/2012 7.00	35.0						05/11/2012 13.00	4.2					
06/10/2012 13.00		33.0	2.1		1.1	4.3	05/11/2012 19.00	6.6	12.6				
06/10/2012 19.00	6.1		1.4	0.9			06/11/2012 1.00	2.6					
07/10/2012 1.00		19.0	7.0		1.8		06/11/2012 7.00	4.1					
07/10/2012 7.00		77.0	2.8		0.5		06/11/2012 13.00	5.4			32.4		
07/10/2012 13.00		8.2	2.0		2.4		06/11/2012 19.00	5.8					
07/10/2012 19.00		19.0	1.6		4.2		07/11/2012 1.00	3.2			56.2		
08/10/2012 1.00	4.4	36.0	1.0	12.8	3.7		07/11/2012 7.00	4.3			43.3		
08/10/2012 7.00	4.1	17.0	2.4		2.5	14.0	07/11/2012 19.00					2.4	
08/10/2012 13.00	7.1	12.0	2.6	13.4	6.3		08/11/2012 1.00		6.4				
08/10/2012 19.00	6.9		5.0	8.7		18.1	08/11/2012 7.00		5.6				
09/10/2012 1.00	8.9		2.6				08/11/2012 13.00	3.1	17.5		15.8		
09/10/2012 7.00	7.3		2.4				08/11/2012 19.00	2.9	9.7				
09/10/2012 13.00	12.5		1.1				09/11/2012 1.00	4.2	7.0				
09/10/2012 19.00	4.6	19.3			5.1		09/11/2012 7.00		4.9				
10/10/2012 1.00	8.9	61.7		4.9	1.3		09/11/2012 13.00	1.0	5.2				
10/10/2012 7.00		40.1			5.1		09/11/2012 19.00	2.1	6.3				
10/10/2012 13.00	5.3	49.9		10.9	2.5		10/11/2012 1.00	2.5	5.4		2.0		
11/10/2012 1.00		50.3			3.2		10/11/2012 7.00	2.9	9.0		2.3		
11/10/2012 7.00		28.7			3.4		10/11/2012 13.00	3.4	9.2				
11/10/2012 19.00	6.6	21.2		14.4	8.0		10/11/2012 19.00	1.3					
12/10/2012 1.00	5.1			4.5			11/11/2012 1.00	4.2					

Table 1. (continued)

Date	CO_2/SO_2			H_2O/CO_2			Date	CO_2/SO_2			H_2O/CO_2		
	VOR	BN	NEC	VOR	BN	NEC		VOR	BN	NEC	VOR	BN	NEC
12/10/2012 7.00	4.4	78.8		12.0	3.5		11/11/2012 7.00	2.2					
12/10/2012 13.00		30.4			2.3		11/11/2012 13.00	2.6					
12/10/2012 19.00	4.6			12.3			11/11/2012 19.00	1.5					
13/10/2012 1.00	3.0	34.9			2.2		12/11/2012 1.00	4.3					
13/10/2012 7.00		35.7			3.6		12/11/2012 7.00	2.2					
13/10/2012 19.00	2.7	49.5		9.1	1.6		12/11/2012 13.00	3.3	9.4		22.4		
14/10/2012 1.00	3.0	62.8			1.1		12/11/2012 19.00	5.2	20.0		13.0	4.8	
14/10/2012 7.00	3.8	37.6		19.1			13/11/2012 1.00	2.3					
14/10/2012 13.00	10.4	64.0		10.6	2.4		13/11/2012 7.00	1.7					
14/10/2012 19.00		18.5			1.6		13/11/2012 13.00	5.3	7.5		8.2		
15/10/2012 1.00		40.5			0.5		13/11/2012 19.00	8.0					
15/10/2012 7.00	6.9	37.0			1.3		14/11/2012 1.00	13.0	7.1				
15/10/2012 19.00	5.8	13.3		27.4	3.5		14/11/2012 13.00	1.8	15.0				
16/10/2012 1.00	1.1			2.8			14/11/2012 19.00	2.4	15.0				
16/10/2012 7.00		41.9			1.9		15/11/2012 1.00	8.5			6.6		
19/10/2012 1.00	4.7	26.7		25.2	3.0		15/11/2012 7.00		48.0				
19/10/2012 7.00	9.1	19.2		11.6	2.1		15/11/2012 19.00		63.0			0.5	
19/10/2012 13.00	2.6	32.0					16/11/2012 7.00	7.2	80.0				
18/11/2012 7.00	6.5	26.0		7.2									
18/11/2012 13.00	4.6	13.8		19.3									
18/11/2012 19.00	5.0			33.6									
19/11/2012 1.00	4.9												
19/11/2012 7.00	3.6			41.7									
19/11/2012 13.00		19.0											
19/11/2012 19.00		15.0											
20/11/2012 1.00	1.6	14.5											
20/11/2012 7.00	3.2			31.9									
20/11/2012 13.00		26.0											
20/11/2012 19.00		44.0			0.9								
21/11/2012 1.00		22.0											
21/11/2012 7.00		11.0											
21/11/2012 13.00		12.5											
21/11/2012 19.00		11.0											
22/11/2012 1.00		31.0											
22/11/2012 7.00		11.8			3.2								
22/11/2012 13.00	16.0	13.7											
23/11/2012 1.00		9.1			3.2								
23/11/2012 7.00	1.3	11.8		5.2	5.9								
23/11/2012 13.00	1.2	10.8		14.7									
23/11/2012 19.00	1.6	11.3											
24/11/2012 1.00	2.0	7.9			1.6								
24/11/2012 7.00		8.6			3.5								
24/11/2012 13.00		11.0			1.8								
24/11/2012 19.00		12.0			5.2								
25/11/2012 1.00		5.0											
25/11/2012 7.00		8.0			4.7								
25/11/2012 13.00	3.1												
26/11/2012 1.00	2.5	11.3											
26/11/2012 7.00	1.9	17.8		2.0									
26/11/2012 13.00	1.4	11.2											
26/11/2012 19.00	1.7	16.9		0.8	0.5								
27/11/2012 1.00	2.1	11.2		4.7									
27/11/2012 7.00	2.7	10.6		1.3									
27/11/2012 13.00	4.2	8.8											
27/11/2012 19.00	1.9												
29/11/2012 1.00		3.9											
29/11/2012 19.00	2.9												
30/11/2012 1.00	2.8			17.8									
13/12/2012 13.00		25.0			4.6								
13/12/2012 19.00		17.0			1.4								
14/12/2012 1.00		10.0			2.7								

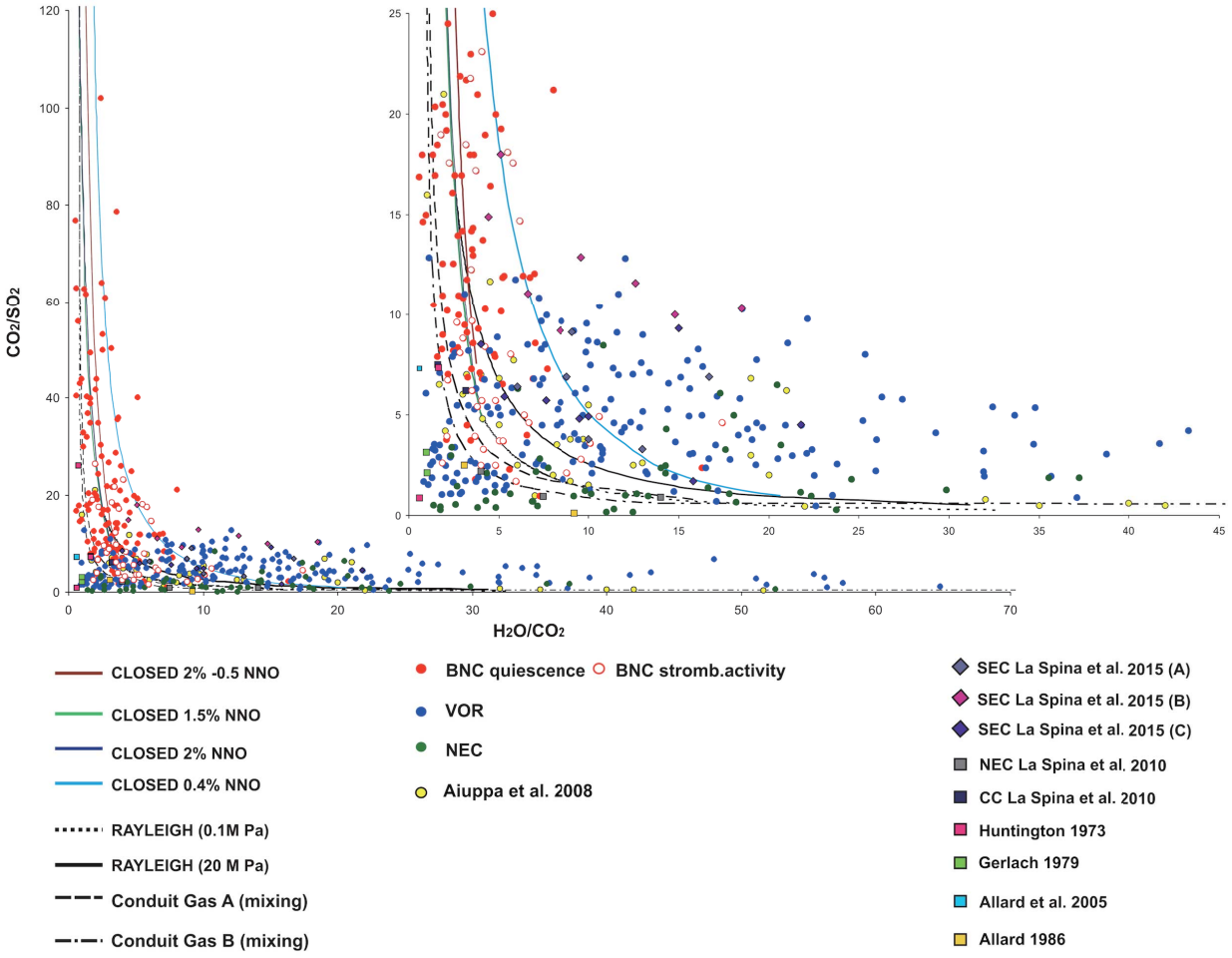

Fig. 5. Scatter plot of (molar) H_2O/CO_2 versus CO_2/SO_2 ratios in the crater plumes of Mount Etna. The summer 2012 data obtained in this study are compared with previously reported H_2O-CO_2-SO_2 gas compositions obtained from various sources. Also shown in the diagram are the results of model runs of volcanic degassing as obtained by using the saturation code Moretti and Papale (2004). The four closed-system curves demonstrate the model evolution of gas composition upon decompression from 200 MPa to 0.1 MPa. The four runs differ for total CO_2 content, from 0.4 wt.% to 2 wt.%, and redox conditions, from NNO to 0.5 log units below NNO. The two open-system curves (indicated as Rayleigh in the legend) describe the evolution of gas separated under isobaric conditions at 0.1 MPa and 20 MPa, respectively, from a melt undergoing crystallization-induced degassing (second boiling). The dashed curves describe the mixing between a 140 MPa-deep reservoir gas and residual conduit gases A and B, which correspond to gases in equilibrium with the cooling of residual magmas in the shallow conduits at 0.1 MPa (Aiuppa et al., 2011).

that observed during quiescence by a factor of ~2, in which the average value was 17 ± 16 at a range of 17–102. For example, a phase of sustained low CO_2/SO_2 ratios was observed during the Strombolian-to-lava-fountaining activity of phase 3 in October 2012, which were the most vigorous explosive events in our observational period. Conversely, the highest CO_2/SO_2 ratios in our dataset were detected in the quiescent periods between episodes 2 and 3 from August 25 to early October 2012; CFR 2). During that time, the BNC was intensely degassing, and only episodic events of ash emissions rich in lithic fragments were observed (INGV-OE; internal reports). It should be noted, however, that the transition from CO_2-poor (eruptive) to CO_2-rich (quiescent) compositions at the BNC were gradual as opposed to sharp and that the CO_2/SO_2 ratios began to increase gradually between episodes III and V of the eruptive phase 2 (Fig. 3).

Similar differences between eruptive and non-eruptive periods were observed at the NEC, with CO_2/SO_2 ratios of 0.8 ± 1 versus 2.7 ± 3, but not at the VOR, in which nearly identical CO_2/SO_2 ratios of 4.6 ± 3.6 versus 4.5 ± 3 were observed in the two distinct phases.

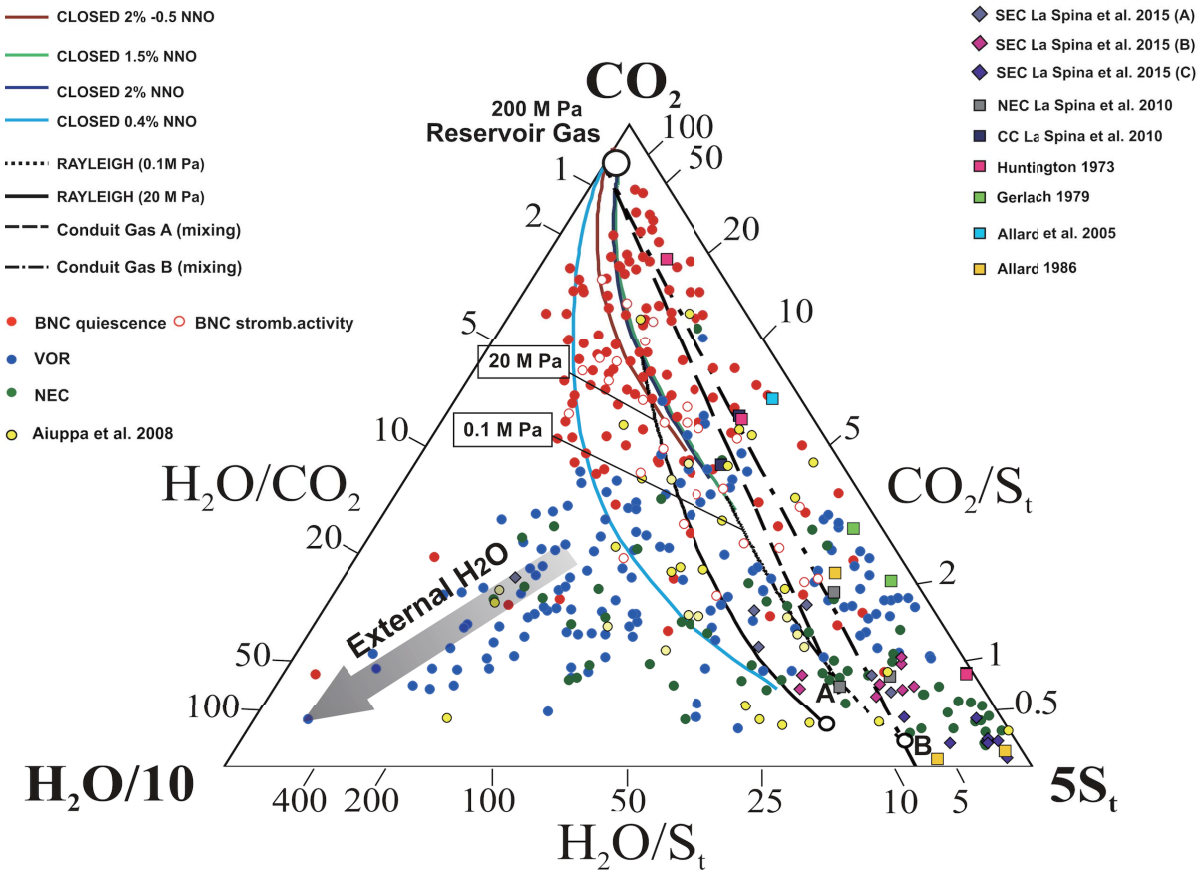

Fig. 6. Triangular plot of H_2O-CO_2-SO_2 relative proportions in the crater plumes of Mount Etna including summer 2012 data derived in this study in addition to that previously reported. H_2O abundances were divided by a factor of 10 and that of SO_2 was multiplied by a factor of 5 for better data representation. The model curves are the same as those described in Fig. 4. The three Etna craters show distinct compositions. Bocca Nuova crater (BNC) gases plot close to the closed-system model lines and can therefore be interpreted as quenched, deep-equilibrium gases extracted from the melt in a pressure range of 200–0.1 MPa. Northeast crater (NEC) and Voragine crater (VOR) gases are more CO_2-poor and SO_2-rich, and are therefore more similar to model gases output by low-pressure (0.1–20 MPa) open-system model runs. A number of VOR gases show a trend of H_2O enrichment that may indicate the involvement of external or meteoric H_2O.

Discussion

Eruptive activity resumed in Mount Etna's BNC CC region in summer 2012 after several years of dormancy. Etna's CCs exhibited frequent, intense terminal eruptive activity during the 1995–2002 eruptive cycle (Allard *et al.*, 2006) and became quiescent excluding vigorously degassing from 2003 to early 2012 when eruptive activity was mainly concentrated in the Southeast (SEC) and New Southeast (NSEC) summit craters (Behncke *et al.*, 2006, 2008, 2009, 2014; Andronico *et al.*, 2008a, b; Liuzzo *et al.*, 2013; Bonaccorso *et al.*, 2011, 2013, 2014; Patanè *et al.*, 2013).

Since it became operative in 2006, the permanent INGV network of Multi-GAS instruments has contributed to interpreting the dynamics of magma movement and degassing beneath the summit region of Etna. By granting more continuous observations with improved temporal resolution over that in periodic surveys (e.g., Aiuppa *et al.*, 2006), the permanent network has allowed for the systematic detection of pulses of CO_2-rich gas discharge weeks or months prior to sub-terminal effusive eruptions, such as the 2006 eruption on the upper southeast flank (Aiuppa *et al.*, 2007), or prior to lava-fountaining activity at the SEC (Aiuppa *et al.*, 2010a) and NSEC (Liuzzo *et al.*, 2013; Patanè *et al.*, 2013). No plume chemistry information relative to Etna's CC activities has been available until the present study.

The results determined in the present study are the first reports for the H_2O-CO_2-SO_2 chemical signature of gas emitted by an Etna CC prior to, during, and after a phase of terminal Strombolian activity. In addition to re-

vealing new information, these new data share a number of similarities with those previously reported (Aiuppa *et al*., 2007, 2010a; Patanè *et al*., 2013).

Similarities with previous work

The 2012 plume results confirm that Etna's various craters are compositionally distinct. As previously documented (Aiuppa *et al*., 2006; Shinohara *et al*., 2008; La Spina *et al*., 2010; Rizzo *et al*., 2015), Etna's CCs, particularly the BNC, emit gas that is typically more CO_2-rich and H_2O-poor than that of the NEC (Figs. 3–5). In view of the deep derivation of CO_2 gas in basaltic systems (Allard, 2010, and references therein), these results imply that the feeding conduits beneath the CCs are the most efficient pathways for gas-bubble transfer from the deep volcano plumbing systems toward the surface (Shinohara *et al*., 2008; La Spina *et al*., 2010). Such preferential gas transport through the BNC feeding conduits is also consistent with seismic recordings of long-period and very-long-period seismicity and seismic tremors, which typically show a cluster of source locations beneath the CCs particularly during quiescent periods (Cannata *et al*., 2009a, b; Patanè *et al*., 2013; Zuccarello *et al*., 2013). The more CO_2-depleted (Fig. 3) and halogen-rich (Aiuppa *et al*., 2005) compositions typically measured at the NEC reflect, in turn, degassing of a more volatile-depleted (bubble-poor) magma. In view of the existing infrasonic (Marchetti *et al*., 2009) and seismological (Di Grazia *et al*., 2009; Patanè *et al*., 2013) evidence of hydraulic connectivity between the craters, models in which the NEC branches from the CC feeding conduit (La Spina *et al*., 2010) so that gas bubbles preferentially flow into the latter may effectively explain the compositional dissimilarities observed at Etna in 2012 and in other periods. Unfortunately, the depth of this branching is poorly constrained; according to model calculations, the range is between 50 MPa and 120 MPa pressure (La Spina *et al*., 2010). The results of the analog models (e.g., Menand and Phillips, 2007) suggest that the extent of gas-bubble segregation in a branch is dependent on several factors including branch geometry, magmatic vesicularity, viscosity, and supply rate. It is highly possible that preferential gas-bubble flow beneath the CCs simply reflects the more vertical geometry of their conduits relative to the more inclined NEC conduit (Menand and Phillips, 2007). Temporal fluctuations in the relative amount of gas bubbles entering the two conduits may effectively reflect changes in the gas-flow rate below the branching (Manga, 1996; Marchetti *et al*., 2009). The VOR, which is located between the BNC and NEC, shows intermediate compositions between the two extremes (Figs. 3–5).

Moreover, the BNC Multi-GAS dataset confirms the extremely mutable nature of plume-gas compositions at Etna that were observed previously (Aiuppa *et al*., 2007, 2010; Patanè *et al*., 2013). CO_2/SO_2 ratios in particular varied at the BNC by approximately two orders of magnitude during only approximately six months of observations (Fig. 3). This large temporal variability contrasts with that reported at less dynamic, mafic volcanic systems such as Miyake-jima and Asama in Japan (Shinohara *et al*., 2003, 2015) and Masaya in Nicaragua (Martin *et al*., 2010) and confirms that variations in the modes and rates of gas-magma ascent and separation are unusually rapid within Etna's shallow plumbing system. We return to quantitative models to explain this temporal variability below. Here, we simply observe that the timing of the CO_2/SO_2 ratio variations examined in this study (Fig. 3) agrees well with the results of Aiuppa *et al*. (2007, 2010a) and Patanè *et al*. (2013). In those previous studies, the cyclic variations of the CC CO_2/SO_2 ratios were identified in which low ratios of <5 were typically observed during eruptive activity at either SEC or NSEC, whereas high ratios of >10 were recurrently detected in the passive plumes released weeks or months prior to the resumption of volcanic activity. Our new results are qualitatively similar such that low-to-intermediate plume CO_2/SO_2 ratios (8.5 ± 6) were associated with periods of Strombolian activity at the BNC during episodes I–V of phase 2 in July–August 2012 and in phase 3 in October 2012 in addition to that during the NSEC activity of November 2012. Conversely, very high ratios of >>10 and occasionally >100 were observed between the eruptive phases, particularly between phases 2 and 3 or during BNC activity, and prior to the November 2012 NSEC eruptive activity (Fig. 3). Unfortunately, no Multi-GAS information is available for the period preceding phase 1 of BNC activity in early July 2012.

Novel implications

A novel and significant outcome of this study is that it allows for the extension of the measured volcanic gas composition ranges at Etna to more CO_2-rich compositions than previously reported. Our results show that a CO_2-rich gas front with exceptionally high CO_2/SO_2 ratios occasionally up to 100 was vented in the BNC by quiescent degassing between phases 2 and 3 of Strombolian activity and before the November 2012 activity of the NSEC. These CO_2/SO_2 compositions are unprecedentedly high in CO_2 for this volcano. For example, the highest CO_2/SO_2 ratio reported by Aiuppa *et al*. (2007) for the CCs prior to and during the summer 2006 SEC Strombolian activity was 45. Similarly, Patanè *et al*. (2013) observed the gas of the CC plumes emitted between 2009 and 2011 and reported that peak values prior to NSEC eruptive episodes never exceeded 30. This comparison shows that compared with the 2006–2011 period, in which Etna's eruptive activity was confined to the upper southeast region, the resumption of eruptive activity

at the CCs is associated with the emission of an unusually CO_2-rich gas from the BNC.

The BNC gas compositions measured in summer 2012 at Etna are also characterized by particularly H_2O-poor compositions. These volcanic gas compositions are compared with previous reports of Etna's gas content in Figs. 4 and 5. Figure 4 confirms the negative relationship between H_2O/CO_2 and CO_2/SO_2 ratios in Etna's gases (Aiuppa *et al*., 2007) and highlights that all of the 2012 $CO_2/SO_2 > 20$ gases have low H_2O/CO_2 ratios <5. The 2012 data plotted along the same compositional array described by previously available H_2O-CO_2-SO_2 gas data from Etna (Aiuppa *et al*., 2007, 2008), although they do extend the previous compositional range to more CO_2- and H_2O-rich compositions. The exceptionally CO_2-rich (and H_2O-poor) composition of the 2012 BNC gas is also supported by the triangular diagram in Fig. 5. Again, our 2012 results only partially overlap with the compositional fields of previous gas data from Etna (Allard *et al*., 2005; Aiuppa *et al*., 2007, 2008; La Spina *et al*., 2010, 2015).

Insights from quantitative modeling

Since the work of Aiuppa *et al*. (2007), the application of multi-component saturation models (Moretti *et al*., 2003; Moretti and Papale, 2004) to volcanic gas datasets has contributed to quantitative interpretation of the degassing processes of Etna. Analogous with the previous work (Aiuppa *et al*., 2007, 2011), we herein use the model of Moretti *et al*. (2003) and Moretti and Papale (2004) to calculate the composition of the magmatic gas in equilibrium with Etnean magmas in a range of pressures (depths) and redox conditions. We then compare the obtained model results with the measured gas compositions shown in Figs. 4 and 5.

As in Aiuppa *et al*. (2007, 2011), all model runs were initialized by setting the temperature at 1100°C. The anhydrous melt composition was set as the average composition of post-1974 trachybasalts, and the total water and sulfur contents were 3.4 wt.% and 0.32 wt.%, respectively (Métrich *et al*., 2004). We conducted several different model runs with distinct initialization parameters. Four runs were operated in closed-system conditions (Figs. 4 and 5) in which the pressure was in all cases varied from 200 MPa down to 0.1 MPa. These runs therefore simulated the evolving composition of gas exsolved by decompressing magmas upon ascent from Etna's deep magma reservoir reported by Spilliaert *et al*. (2006). The closed-system runs had distinct total CO_2 contents of 0.4, 1.5, and 2 wt.%, respectively, and redox conditions from the NNO buffer to 0.5 log units below NNO (Aiuppa *et al*., 2011), to explore the manner in which these less-constrained parameters affect the simulation results. Our model results (Figs. 4 and 5) indicate that at least in the explored range of melt-oxidation states, the CO_2 contents play a larger role in model degassing trends than redox trends. The two Rayleigh-type open-system runs (Figs. 4 and 5) are the same as those in Aiuppa *et al*. (2007) and were calculated at constant pressures of 0.1 MPa and 20 MPa, respectively. These model trends therefore represent the gas exsolved in isobaric conditions by increasing the degassing extents of a crystallizing magma. Finally, also shown in Figs. 4 and 5 are the modeled gas mixtures from Aiuppa *et al*. (2011) between (i) a deep reservoir gas in equilibrium with Etna's basalt at 1100°C and 140 MPa pressure and (ii) two distinct conduit gases (A and B of Aiuppa *et al*., 2011) in equilibrium with the Etna's shallow conduit magma at 0.1 MPa pressure.

The comparison of model results and natural data (Figs. 4 and 5) demonstrates that BNC gas compositions are in overall agreement with the model predictions of closed-system runs. In particular, the exceptionally CO_2-rich compositions of quiescent BNC emissions, such as those measured between phases 2 and 3 of BNC Strombolian activity, qualitatively match the modeled magmatic gas compositions returned by closed-system model runs in the 150–15 MPa pressure range. This match between the model results and observations supports the conclusion that a major surge of deeply sourced gas pervaded the shallow plumbing system of the CCs in summer 2012 and was passively vented at the surface through the plume between episodes of Strombolian activity. Based on our model simulations, we contend that gases originating from the deep magma storage, reported by Spilliaert *et al*. (2006) as 220–170 MPa 6–4 km below sea level, may have sourced Etna's pre-eruptive plume degassing in summer 2012. In contrast, the BNC gases vented during active Strombolian degassing were generally more CO_2-poor and H_2O-SO_2-rich, with some overlap between active and passive BNC gas compositions. The characteristics of these gases are closer to the modeled gas compositions calculated in either closed- or open-system conditions at lower pressure <15 MPa and in most cases ~0.1 MPa. This result confirms the shallow gas provenance, from syn-eruptive magmatic degassing, of the H_2O-SO_2-richer gas vented during active Strombolian phases. The gas compositions observed at the NEC during summer 2012 were systematically more CO_2-depleted compared with the modeled gas compositions formed by bulk (closed-system) magmatic degassing at 0.1 MPa pressure. These gases are more similar in composition to the modeled conduit gases formed by the residual degassing of bubble-free crystallizing magmas. This observation confirms that bubble-depleted gases filled the NEC-branched conduit system (La Spina *et al*., 2010). Finally, the gas compositions measured at the VOR were intermediate between those observed at the BNC and NEC, indicating that a moderately degassed, residual magma prevailed at this crater during summer 2012. The

tendency of numerous VOR gas samples toward the H_2O corner (Fig. 5) suggests the possible involvement of external or meteoric water in the degassing budget of this crater. This conclusion is consistent with the recurrent observation of low temperatures inside the VOR crater obtained by thermal infrared (IR) monitoring (INGV-OE activity reports) and indicates the possible obstruction of the vent, which favors interaction with meteoric fluids (Liotta *et al*., 2010; Aiuppa *et al*., 2011). Despite the recurrent H_2O-rich nature of the VOR gas, we detected no evidence of SO_2 loss due to in-plume condensation processes.

Conclusions

We have shown in this study that the resumption of Strombolian activity at Etna CCs in summer 2012 was accompanied by discharge of the most CO_2-rich gas ever observed at this volcano. The unprecedented high CO_2/SO_2 ratios >100 observed at BNC, interpreted through model simulations of magmatic degassing, suggest that a major pulse of deeply derived (P > 100 MPa) gas, likely supplied by the deep volcano's plumbing system, was injected into the shallow CC conduits and was vented in quiescent form at the BNC between eruptive episodes. In view of the rather evolved nature of magmas that erupted during the BNC 2012 activity (INGV-OE activity reports) and in line with recent work (Paonita *et al*., 2012; Patanè *et al*., 2013; Ferlito *et al*., 2014), we tentatively propose that these gas bubbles of deep origin rejuvenated resident magma present in Etna's shallow plumbing system and forced its eruption in the BNC during summer 2012 activity. Moreover, sin-eruptive, shallow magmatic degassing of S and H_2O dissolved in this resident magma contributed to the SO_2-H_2O-rich gas that erupted during Strombolian activity episodes.

Acknowledgments—The research leading to these results has received funding from the European Research Council under the European Union's Seventh Framework Programme (FP7/2007/2013)/ERC grant agreement n 305377. F. Ciancitto kindly provided an illustration of intra-crateric Strombolian activity at BNC crater (Fig. 2), and G. Salerno is acknowledged for providing a copy of Etna's digital elevation model (DEM; Fig. 1). T. Pering and an anonymous reviewer are acknowledged for providing constructive comments.

References

Aiuppa, A., Allard, P., D'Alessandro, W., Giammanco, S., Parello, F. and Valenza, M. (2004) Magmatic gas leakage at Mount Etna (Sicily, Italy): Relationship with volcano-tectonic structures, the hydrological pattern and the eruptive activity. *Etna Volcano Laboratory* **143** (Bonaccorso, A., Calvari, S., Coltelli, M., Del Negro, C. and Falsaperla, S., eds.), 129–143, AGU.

Aiuppa, A., Inguaggiato, S., McGonigle, A. J. S., O'Dwyer, M., Oppenheimer, C., Padgett, M. J., Rouwet, D. and Valenza, M. (2005) H_2S fluxes from Mt. Etna, Stromboli, and Vulcano (Italy) and implications for the sulfur budget at volcanoes. *Geochim. Cosmochim. Acta* **69**, 1861–1871.

Aiuppa, A., Federico, C., Giudice, G., Gurrieri, S., Liuzzo, M., Shinohara, H., Favara, R. and Valenza, M. (2006) Rates of carbon dioxide plume degassing from Mount Etna volcano. *J. Geophys. Res*. **111**, doi:10.1029/2006JB004307.

Aiuppa, A., Moretti, R., Federico, C., Giudice, G., Gurrieri, S., Liuzzo, M., Papale, P., Shinohara, H. and Valenza, M. (2007) Forecasting Etna eruption by real-time observation of volcanic gas composition. *Geology* **35**, 1115–1118.

Aiuppa, A., Giudice, G., Gurrieri, S., Liuzzo, M., Burton, M., Caltabiano, T., McGonigle, A. J. S., Salerno, G., Shinohara, H. and Valenza, M. (2008) Total volatile flux from Mount Etna. *Geophys. Res. Lett*. **35**, doi:10.1029/2008GL035871.

Aiuppa, A., Cannata, A., Cannavò, F., Di Grazia, G., Ferrari, F., Giudice, G., Gurrieri, S., Liuzzo, M., Mattia, M., Montalto, P., Patanè, D. and Puglisi, G. (2010a) Patterns in the recent 2007–2008 activity of Mount Etna volcano investigated by integrated geophysical and geochemical observations. *Geochem. Geophys. Geosyst*. **11**(9), doi:10.1029/2010GC003168.

Aiuppa, A., Burton, M., Caltabiano, T., Giudice, G., Guerrieri, S., Liuzzo, M., Muré, F. and Salerno, G. (2010b) Unusually large magmatic CO_2 gas emissions prior to a basaltic paroxysm. *Geophys. Res. Lett*. **37**, doi:10.1029/2010GL043837.

Aiuppa, A., Shinohara, H., Tamburello, G., Giudice, G., Liuzzo, M. and Moretti, R. (2011) Hydrogen in the gas plume of an open-vent volcano, Mount Etna, Italy. *J. Geophys. Res*. **116**, doi:10.1029/2011JB008461.

Aiuppa, A., Robidoux, P., Tamburello, G., Conde, V., Galle, B., Avard, G., Bagnato, E., DeMoor, J. M., Martínez, M. and Muñóz, A. (2014) Gas measurements from the Costa Rica-Nicaragua volcanic segment suggest possible along-arc variations in volcanic gas chemistry. *Earth Planet. Sci. Lett*. **407**, 134–147.

Allard, P. (1986) Geochimique isotopique et origine de l'eau, du carbon, et du sufre dans le gaz volcanique: zone de rift, marges continentales et acrs insulaires. Ph.D. Thesis, Univ Paris 7, Paris.

Allard, P. (2010) A CO_2-rich gas trigger of explosive paroxysms at Stromboli volcano, Italy. *J. Volcanol. Geotherm. Res*. **189**, 363–374.

Allard, P., Carbonnelle, J., Dajlevic, D., Le Bronec, J., Morel, P., Robe, M. C., Maurenas, J. M., Faivrepierret, R., Martin, D., Sabroux, J. C. and Zettwoog, P. (1991) Eruptive and diffuse emissions of CO_2 from Mt. Etna. *Nature* **351**, 387–390.

Allard, P., Burton, M. and Muré, F. (2005) Spectroscopic evidence for a lava fountain driven by previously accumulated magmatic gas. *Nature* **433**, 407–410.

Allard, P., Behncke, B., D'Amico, S., Neri, M. and Gambino, S. (2006) Mount Etna 1993–2005: Anatomy of an evolving eruptive cycle. *Earth Sci. Rev*. **78**, 85–114.

Andronico, D., Scollo, S., Caruso, S. and Cristaldi, A. (2008a)

The 2002–03 Etna explosive activity: Tephra dispersal and features of the deposits. *J. Geophys. Res*. **113**, 1–16.

Andronico, D., Cristaldi, A. and Scollo, S. (2008b) The 4–5 September 2007 lava fountain at South-East Crater of Mt. Etna, Italy. *J. Volcanol. Geotherm. Res*. **173**, 325–328.

Behncke, B., Neri, M., Pecora, E. and Zanon, V. (2006) The exceptional activity and growth of the Southeast Crater, Mount Etna (Italy), between 1996 and 2001. *Bull. Volcanol*. **69**, 149–173.

Behncke, B., Calvari, S., Giammanco, S., Neri, M. and Pinkerton, H. (2008) Pyroclastic density currents resulting from the interaction of basaltic magma with hydrothermally altered rock: an example from the 2006 summit eruptions of Mount Etna, Italy. *Bull. Volcanol*. **70**, 1249–1268.

Behncke, B., Falsaperla, S. and Pecora, E. (2009) Complex magma dynamics at Mount Etna revealed by seismic, thermal, and volcanological data. *J. Geophys. Res*. **114**, doi:10.1029/2008JB005882.

Behncke, B., Branca, S., Corsaro, R. A., De Beni, E., Miraglia, L. and Proietti, C. (2014) The 2011–2012 summit activity of Mount Etna: Birth, growth and products of the new SE crater. *J. Volcanol. Geotherm. Res*. **270**, 10–21.

Bonaccorso, A., Calvari, S., Coltelli, M., Del Negro, C. and Falsaperla, S. (2004) *Etna Volcano Laboratory* **143** (Bonaccorso, A., Calvari, S., Coltelli, M., Del Negro, C. and Falsaperla, S., eds.), 143–369, AGU.

Bonaccorso, A., Caltabiano, T., Currenti, G., Del Negro, C., Gambino, S., Ganci, G., Giammanco, S., Greco, F., Pistorio, A., Salerno, G., Spampinato, S. and Boschi, E. (2011) Dynamics of a lava fountain revealed by geophysical, geochemical and thermal satellite measurements: the case of the 10 April 2011 Mt. Etna eruption. *Geophys. Res. Lett*. **38**, doi:10.1029/2011GL049637.

Bonaccorso, A., Calvari, S., Currenti, G., Del Negro, C., Ganci, G., Linde, A., Napoli, R., Sacks, S. and Sicali, A. (2013) From source to surface: dynamics of Etna's lava fountains investigated by continuous strain, magnetic, ground and satellite thermal data. *Bull. Volcanol*. **75**, 690, doi:10.1007/s00445-013-0690-9.

Bonaccorso, A., Calvari, S., Linde, A. and Sacks, S. (2014) Eruptive processes leading to the most explosive lava fountain at Etna volcano: The 23 November 2013 episode. *Geophys. Res. Lett*. **41**(14), 4912–4919.

Bonforte, A., Bonaccorso, A., Guglielmino, F., Palano, M. and Puglisi, G. (2008) Feeding system and magma storage beneath Mt. Etna as revealed by recent inflation/deflation cycles. *J. Geophys. Res*. **113**, doi:10.1029/2007JB005334.

Caltabiano, T., Burton, M., Giammanco, S., Allard, P., Bruno, N., Muré, F. and Romano, R. (2004) Volcanic gas emissions from the summit craters and flanks of Mt. Etna, 1987–2000. *Etna Volcano Laboratory* **143** (Bonaccorso, A., Calvari, S., Coltelli, M., Del Negro, C. and Falsaperla, S., eds.), 111–126 AGU.

Cannata, A., Montalto, P., Privitera, E., Russo, G. and Gresta, S. (2009a) Tracking eruptive phenomena by infrasound: May 13, 2008, eruption at Mt. Etna. *Geophys. Res. Lett*. **36**, 6–11.

Cannata, A., Montalto, P., Privitera, E. and Russo, G. (2009b) Characterization and location of infrasonic sources in active volcanoes: Mount Etna, September–November 2007. *J. Geophys. Res*. **114**, 1–15.

Di Grazia, G., Cannata, A., Montalto, P., Patanè, D., Privitera, E., Zuccarello, L. and Boschi, E. (2009) A multiparameter approach to volcano monitoring based on 4D analyses of seismo-volcanic and acoustic signals: the 2008 Mt. Etna eruption. *Geophys. Res. Lett*. **36**, 2–7.

Ferlito, C., Coltorti, M., Lanzafame, G. and Giacomoni, P. P. (2014) The volatile flushing triggers eruptions at open conduit volcanoes: Evidence from Mount Etna volcano (Italy). *Lithos* **184–187**, 447–455.

Francis, P., Burton, M. R. and Oppenheimer, C. (1998) Remote measurements of volcanic gas compositions by solar occultation spectroscopy. *Nature* **396**, 567–570.

Gerlach, T. M. (1979) Evaluation and restoration of the 1970 volcanic gas analyses from Mt Etna. *J. Volcanol. Geotherm. Res*. **6**, 165–178

Gerlach, T. M. (1991) Present-day CO_2 emissions from volcanoes. *Eos Trans. AGU* **72**, 249–256.

Huntington, A. T. (1973) The collection and analysis of volcanic gases from Mt Etna. *Phil. Trans. R. Soc. London* **27aA**, 119–128.

La Spina, A., Burton, M. and Salerno, G. G. (2010) Unravelling the processes controlling gas emissions from the central and northeast craters of Mt. Etna. *J. Volcanol. Geotherm. Res*. **198**, 368–376.

La Spina, A., Burton, M., Allard, P., Alparone, S. and Muré, F. (2015) Open-path FTIR spectroscopy of magma degassing processes during eight lava fountains on Mount Etna. *Earth Planet. Sci. Lett*. **413**, 123–134.

Liotta, M., Paonita, A., Caracausi, A., Martelli, M., Rizzo, A. and Favara, R. (2010) Hydrothermal processes governing the geochemistry of the crater fumaroles at Mount Etna volcano (Italy). *Chem. Geol*. **278**, 92–104.

Liuzzo, M., Gurrieri, S., Giudice, G. and Giuffrida, G. (2013) Ten years of soil CO_2 continuous monitoring on Mt. Etna: Exploring the relationship between processes of soil degassing and volcanic activity. *Geochem. Geophys. Geosyst*. **14**, 2886–2899.

Manga, M. (1996) Dynamics of drops in branched tubes. *J. Fluid Mech*. **315**, 105–117.

Marchetti, E., Ripepe, M., Ulivieri, G., Caffo, S. and Privitera, E. (2009) Infrasonic evidences for branched conduit dynamics at Mt. Etna volcano, Italy. *Geophys. Res. Lett*. **36**, 1–5.

Martelli, M., Caracausi, A., Paonita, A. and Rizzo, A. (2008) Geochemical variations of air-free crater fumaroles at Mt. Etna: New inferences for forecasting shallow volcanic activity. *Geophys. Res. Lett*. **35**, 2–7.

Martin, R. S., Sawyer, G. M., Spampinato, L., Salerno, G. G., Ramirez, C., Ilyinskaya, E., Witt, M. L. I., Mather, T. A., Watson, I. M., Phillips, J. C. and Oppenheimer, C. (2010) A total volatile inventory for Masaya Volcano, Nicaragua. *J. Geophys. Res*. **115**, doi:10.1029/2010JB007480.

Menand, T. and Phillips, J. C. (2007) Gas segregation in dykes and sills. *J. Volcanol. Geotherm. Res*. **159**, 393–408.

Métrich, N., Allard, P., Spilliaert, N., Andronico, D. and Burton, M. (2004) 2001 flank eruption of the alkali- and volatile-rich primitive basalt responsible for Mount Etna's evolution in the last three decades. *Earth Planet. Sci. Lett*. **228**,

1–17.

Moretti, R. and Papale, P. (2004) On the oxidation state and volatile behavior in multicomponent gas-melt equilibria. *Chem. Geol*. **213**, 265–280.

Moretti, R., Papale, P. and Ottonello, G. (2003) A model for the saturation of C-O-H-S fluids in silicate melts. *Geol. Soc. London Spec. Pub*. **213**, 81–101.

Paonita, A., Caracausi, A., Iacono-Marziano, G., Martelli, M. and Rizzo, A. (2012) Geochemical evidence for mixing between fluids exsolved at different depths in the magmatic system of Mt. Etna (Italy). *Geochim. Cosmochim. Acta* **84**, 380–394.

Patanè, D., Aiuppa, A., Aloisi, M., Behncke, B., Cannata, A., Coltelli, M., Di Grazia, G., Gambino, S., Gurrieri, S., Mattia, M. and Salerno, G. (2013) Insights into magma and fluid transfer at Mount Etna by a multiparametric approach: A model of the events leading to the 2011 eruptive cycle. *J. Geophys. Res*. **118**, 3519–3539.

Pering, T. D., Tamburello, G., McGonigle, A. J. S., Aiuppa, A., Cannata, A., Giudice, G. and Patanè, D. (2014) High time resolution fluctuations in volcanic carbon dioxide degassing from Mount Etna. *J. Volcanol. Geotherm. Res*. **270**, 115–121.

Pering, T. D., Tamburello, G., McGonigle, A. J. S., Aiuppa, A., James, M. R., Lane, S. J., Sciotto, M., Cannata, A. and Patanè, D. (2015) Dynamics of mild strombolian activity on Mt. Etna. *J. Volcanol. Geotherm. Res*. **300**, 103–111 (http://dx.doi.org/10.1016/j.jvolgeores.2014.12.013).

Rizzo, A. L., Liuzzo, M., Ancellin, M. A. and Jost, H. J. (2015) Real-time measurements of $\delta^{13}C$, CO_2 concentration, and CO_2/SO_2 in volcanic plume gases at Mount Etna, Italy, over 5 consecutive days. *Chem. Geol*. **411**, 182–191.

Shinohara, H. (2013) Volatile flux from subduction zone volcanoes: Insights from a detailed evaluation of the fluxes from volcanoes in Japan. *J. Volcanol. Geotherm. Res*. **268**, 46–63.

Shinohara, H., Fukui, K., Kazahaya, K. and Saito, G. (2003) Degassing process of Miyakejima volcano: implications of gas emission rate and melt inclusion data. *Melt Inclusions in Volcanic Systems. Advances in Volcanology* **4**, 147–161.

Shinohara, H., Aiuppa, A., Giudice, G., Gurrieri, S. and Liuzzo, M. (2008) Variation of H_2O/CO_2 and CO_2/SO_2 ratios of volcanic gases discharged by continuous degassing of Mount Etna volcano, Italy. *J. Geophys. Res*. **113**, 1–11.

Shinohara, H., Ohminato, T., Takeo, M., Tsuji, H. and Kazahaya, R. (2015) Monitoring of volcanic gas composition at Asama volcano, Japan, during 2004–2014. *J. Volcanol. Geotherm. Res*. **303**, 199–208.

Spilliaert, N., Allard, P., Métrich, N. and Sobolev, V. (2006) Melt inclusion record of the conditions of ascent, degassing, and extrusion of volatile-rich alkali basalt during the powerful 2002 flank eruption of Mount Etna (Italy). *J. Geophys. Res*. **111**, doi:10.1029/2005JB003934.

Tamburello, G. (2015) Ratiocalc: software for processing data from multicomponent volcanic gas analyzers. *Comput. Geosci*. **82**, 63–67.

Zuccarello, L., Burton, M. R., Saccorotti, G., Bean, C. J. and Patanè, D. (2013) The coupling between very long period seismic events, volcanic tremor, and degassing rates at Mount Etna volcano. *J. Geophys. Res*. **118**, 4910–4921.